Asymptotic scaling properties and estimation of the Generalized Hurst Exponents in financial data

R. J. Buonocore,[1,*] T. Aste,[2,3] and T. Di Matteo[1,2]

[1] *Department of Mathematics, King's College London, The Strand, London, WC2R 2LS, UK*
[2] *Department of Computer Science, University College London, Gower Street, London, WC1E 6BT, UK*
[3] *Systemic Risk Centre, London School of Economics and Political Sciences, London, WC2A2AE, UK*

Abstract

We propose a new method to measure the Hurst exponents of financial time-series. The scaling of the absolute moments against the aggregation horizon of real financial processes and of both uniscaling and multiscaling synthetic processes converges asymptotically towards linearity in log-log scale. In light of this we found appropriate a modification of the usual scaling equation via the introduction of a filter function. We devised a measurement procedure which takes into account the presence of the filter function without the need of directly estimating it. We verified that the method is unbiased within the errors by applying it to synthetic time-series with known scaling properties. Finally we show an application to empirical financial time-series where we fit the measured scaling exponents via a second or a fourth degree polynomial, which, thanks to theoretical constraints have respectively only one and two degrees of freedom. We found that on our dataset there is not clear preference among the second or fourth degree polynomial. Moreover the study of the filter functions of each time-series shows common patterns of convergence depending on the momentum degree.

* riccardo_junior.buonocore@kcl.ac.uk

I. INTRODUCTION

The multifractal behaviour of the financial time-series is one of the acknowledged stylized facts in the literature (see: [1–5]). Many works have been dedicated to its empirical characterization [6–23], reporting strong evidence of its presence in financial markets. Several models have been proposed [24–33] to reproduce these empirical facts.

Multifractality proved to be a very valuable tool. From a theoretical point of view models with a multifractal nature display also power law tails and volatility clustering, leading to consider these well-known stylized facts as consequences of the multifractal nature of financial time-series. From a practical point of view multifractal models proved to have also forecasting power [26, 34–36].

Many estimation methods are present in the literature, in particular the most popular are: Multifractal Detrended Fluctuation Analyisis (MFDFA) [37], Generalized Hurst Exponent Method (GHE) [4, 38–40] and Wavelet Transform Modulus Maxima (WWTM) [41]. All of them have advantages and drawbacks: the MFDFA, which measures the scaling of the so-called fluctuation function, is applicable to non-stationary time-series but the degree of the detrending method is arbitrary; the GHE computes directly the scaling of the moments with respect to the aggregation horizon but the measurements are aggregation horizon dependent; the WWTM has a deep mathematical formulation which makes a parallelism with the thermodynamic, computes the scaling of a partition function defined in terms of WTMM coefficients but the choice of the wavelet function is arbitrary again. Moreover all these methods deal with the study of the scaling of a certain quantity against another one but none of them gives a prescription on how to properly choose the scaling region and why certain regions should be discarded.

The aim of this paper is to propose a new method for the estimation of the scaling behaviour of the moments of real financial time-series with respect to the aggregation horizon, without the need of free parameters and which gives a precise prescription of the scaling region which has to be considered. In a previous paper [42], solving an ongoing debate in the literature (see for example [43–45]), it has been clarified that the true source of the multifractal behaviour found in empirical financial time-series is their causal structure. However it was also shown that the measure of multifractality performed via the scaling of the moments in log-log scale is aggregation horizon dependent and that the true multifractal scaling should be measured in the limit of infinite aggregation horizon. In particular, already for processes with i.i.d. increments but with power law tails in their distribution with exponents between 2 and 5, which is the range empirically observed [46], due to the slow convergence of the Central Limit Theorem the small aggregation horizon is affected by strong biases [42]. In light of this, we now face the problem of building up an estimation procedure able to address these issues and to reduce as much as possible these biases by proposing a reliable proxy of the asymptotic multifractal behaviour of real financial time-series. For reason that are detailed later in the paper the method is well-suited for intraday high frequency data, in particular in this paper we focus on tick-by-tick data.

The structure of the paper is as follows: in Sec. II we recall the geometrical and statistical definitions of multifractality, in Sec. III we discuss the main features of the models we use in the paper to validate the proposed method, in Sec. IV we discuss the effect of the discreteness of processes on scaling measures, in Sec. V we introduce the method, in Sec. VI we show a step by step application of the method on a synthetic process with known multifractal properties, in Sec. VII we perform first a step by step application of the method to one real financial time-series then we apply it to different real time-series and in Sec. VIII we draw the conclusions.

II. MULTIFRACTALITY

In this section we give an overview on what is multifractality from a mathematical point of view giving its geometrical and statistical characterization.

A. Geometrical characterization

Let $X(t)$ be a process continuous in time with stationary increments. The notion of local Hölder exponent $h(t)$ can be introduced via the following expression [47]

$$|X(t+dt) - X(t)| \sim C(t)(dt)^{h(t)}, \tag{1}$$

where $C(t)$ is a function of t and dt is an infinitesimal quantity which tends to zero. Also, in order to assure that stationarity holds almost surely, the set on which $C(t)$ and $h(t)$ vary has zero Lebesgue measure. Intuitively the local Hölder exponent quantifies the local degree of singularity of a time-series [47]. The set of all local Hölder exponents thus expresses the degree of singularity of the whole process $X(t)$ associating a number at every point in time. In

order to characterize the distribution of the local Hölder exponents, the notion of *Singularity Spectrum* $D(h)$ was introduced (cfr. [47–50]). It is defined, for a given value $\bar{h}$, as

$$D(\bar{h}) = D_H\{t : h(t) = \bar{h}\}, \tag{2}$$

where D_H means the Hausdorff (or fractal) dimension of the set in curly brackets. So the Singularity Spectrum codifies the fractal dimension of the points sharing the same degree of singularity (Hölder exponent)[1] [47–50][2]. If only one Hölder exponent, say h_0, characterizes the process, then the process is said to be mono or uni-fractal and the Singularity Spectrum reads as [51]

$$D(h) = \begin{cases} 1 & h = h_0 \\ -\infty & \text{otherwise,} \end{cases} \tag{3}$$

so the spectrum reduces to a single point. A process is said to be multifractal if it has a range of values of h over which $D(h) \geq 0$ [47, 51].

B. Statistical characterization

It turned out that the geometrical properties of a process can be linked to its statistical ones. In particular the so called Multifractal Formalism was introduced [48–50] and can be applied in the context of the stochastic processes [47]. Taking again the stationary, continuous in time, process $X(t)$ and computing its increments over a time horizon τ, it can be shown that, if the following scaling relation holds [52]

$$E[|X(t+\tau) - X(t)|^q] = K(q)\tau^{\zeta(q)}, \tag{4}$$

where both $K(q)$ and $\zeta(q)$ are functions of q and $\zeta(q)$ is concave [24], then $D(h)$ and $\zeta(q)$ are simply linked via a Legendre transform (see for example [5, 47]), namely

$$\zeta(q) = 1 + \inf_h\{qh - D(h)\}, \tag{5}$$

$$D(h) = 1 + \inf_q\{hq - \zeta(q)\}. \tag{6}$$

The request of concavity is crucial for this result since otherwise the Legendre Transform would not be well-defined.

In practical situation one does not deal with processes in time. As a consequence, it was shown [5, 48] that the straightforward estimation of $D(h)$ cannot be practically achieved. In light of this, the importance of relations (5) and (6) relies in the fact that they allow to estimate a geometrical quantity (the Singularity Spectrum) via statistical measurements. In particular one assumes that a real process (for example a log-price) is a discretized version of an underlying unobservable process continuous in time, which are sharing the same statistical properties. Thus, while geometrical arguments cannot be applied to the discrete version, statistical ones are. Usually the function $\zeta(q)$ is rewritten as $\zeta(q) = qH(q)$, with $H(q)$ called the Generalized Hurst Exponent [4, 38, 39]. In particular, from Eq. (6) (in order to find the minimum) we obtain the following chain of equalities

$$h = \frac{d\zeta(q)}{dq} = H(q) + q\frac{dH(q)}{dq}, \tag{7}$$

which shows that the Hölder exponent is equal to the Hurst exponent only when the latter does not depend on q, which is the case of unifractal time-series where $\zeta(q)$ reduces to a straight line. The two most notable unifractal processes are the Brownian Motion (BM) and the Fractional Brownian Motion (fBM), which satisfy respectively $\zeta(q) = q/2$, thus $H(q) = 0.5$, and $\zeta(q) = qH$, thus $H(q) = H$ (see for example [4]).

III. MODELS

In this section we summarize the main properties of the synthetic processes we use throughout the paper in order to validate the new method we introduce in Sec. V.

---

[1] This implies $0 \leq D(H) \leq 1$.

[2] We report that in [47, 51] other two definitions can be found.

A. Brownian Motion with t-Student innovations (tBM)

We here introduce a uniscaling process with i.i.d. increments drawn from a t-Student distribution. Using the dummy variable t, we can write the probability density of a t-Student distribution as (see for example [53])

$$p(t) = \frac{\Gamma(\frac{n+1}{2})}{\sqrt{n\pi}\Gamma(\frac{n}{2})}\left(1+\frac{t^2}{n}\right)^{-\left(\frac{n+1}{2}\right)}, \tag{8}$$

where $\Gamma(\cdot)$ is the gamma function and n is the number of degrees freedom which are allowed to be non-integer. According to Eq. (8) if $n > 1$ the variable t has mean zero, otherwise it is infinite. The variance instead equals $\frac{n}{n-2}$ if $n > 2$, infinite if $1 < n < 2$ and it is undefined otherwise. As for the spectrum of a tBM, it can be computed analytically in both cases, either if n is bigger or smaller than two. When $n < 2$ the t-Student distribution of Eq. (8) becomes a stable distribution with skewness parameter equal to zero and stability parameter equal to n. So its scaling exponents can be readily written as (see [37, 54, 55])[3]

$$\zeta(q) = qH(q) = \frac{q}{n} \quad \text{if } q < n. \tag{9}$$

For $n > 2$ and finite aggregation horizon τ it can be shown, as a corollary of the *Central Limit Theorem* (CLT), that

$$E[|X(t+\tau) - X(t)|^q] = f(q)\tau^{\frac{q}{2}}, \tag{10}$$

where $f(q)$ is a function of q. Thus

$$\zeta(q) = qH(q) = \frac{q}{2}. \tag{11}$$

For $n > 2$ the absolute moments of a tBM scale as those of a BM. For $n = 2$, it can be proved rigorously that the scaling exponents behave like Eq. (11) (cfr. [56]).

Summarizing, a tBM is a unifractal process both for $n < 2$ and $n \geq 2$ with $\zeta(q)$ behaving as a straight line with slopes respectively $1/n$ and $1/2$.

B. Multifractal Random Walk (MRW)

Different multifractal models have been proposed in the literature, however in the present paper we chose as our benchmark multifractal model the so-called Multifractal Random Walk introduced in [30] since it has exactly computable scaling exponents. Despite further developement and alternative multifractal random walks models with different scaling exponents have been proposed (see [32, 33]), for our purposes the statistical properties of this original model are sufficient. The process $X(t)$ described by the model is defined as the limit $\Delta t \to 0$ of the discretization step Δt of (see [30])

$$X(t) = \sum_{k=1}^{\frac{t}{\Delta t}} \epsilon_{\Delta t}(k) e^{\omega_{\Delta t}(k)}, \tag{12}$$

with $\epsilon_{\Delta t} \sim N(0, \sigma^2\Delta t)$, $\omega_{\Delta t} \sim N(-\lambda^2 \ln(L/\Delta t), \lambda^2 \ln(L/\Delta t))$, where λ is called intermittency parameter, L is the autocorrelation length and σ is the variance of the overall process [30]. The increments of this process can then be written as

$$r_\tau(t) = X(t+\tau) - X(t) = \sum_{k=\frac{t}{\Delta t}+1}^{\frac{t+\tau}{\Delta t}} \epsilon_{\Delta t}(k) e^{\omega_{\Delta t}(k)}, \tag{13}$$

.

[3] In [37] the shape of the scaling exponent for $q > n$ is reported to be equal to one. However, as underlined in [54] and [55], this so-called bifractal behaviour is a pure finite size sample effect.

What charaterizes this model is that autocorrelation structure, in particular the $\epsilon_{\Delta t}(k)$ are i.i.d and the $\omega_{\Delta t}(k)$ are not, having autocovariance (see [30]):

$$Cov(\omega_{\Delta t}(k_1), \omega_{\Delta t}(k_2)) = \lambda^2 \ln \rho_{\Delta t}(k_1 - k_2), \tag{14}$$

with

$$\rho_{\Delta t}(k_1 - k_2) = \begin{cases} \dfrac{L}{(|k_1 - k_2| + 1)\Delta t} & |k_1 - k_2| < L/\Delta t, \\ 1 & \text{otherwise.} \end{cases} \tag{15}$$

The scaling exponents of this model in the continuous time limit are (see [30]):

$$\zeta(q) = qH(q) = -\frac{\lambda^2}{2} q^2 + (\lambda^2 + \frac{1}{2})q. \tag{16}$$

What makes this model very appealing for statistical testing is that it exhibits both power law tails and volatility clustering, keeping its plain innovations uncorrelated despite in its definition only three parameters (λ, L, σ) appear. In particular the intermittency parameter λ determines both the power law tails, which decay with an exponent proportional to λ^2 (see [57]), and the decay of the autocorrelation functions of the powers of the absolute returns, whose decaying exponents are again proportional to λ^2 (see [30]).

IV. THE CURSE OF THE DISCRETIZATION

As underlined in Subsec. II B the introduction of the multifractal formalism allows to study the geometrical fractal properties of a process by analysing its discrete version. However, as shown in [42], the estimation of the scaling exponents turned out to be strongly biased. Convergence issues arise for both power law-tailed and autocorrelated discrete processes, both for synthetic and real data. In this section we discuss in more detail these two features in the case of synthetic processes, which in turn will justify our choice of introducing the filter function in Sec. V. The need of the filter function also for real financial process will become evident in Sec. VII where we apply our method to real data.

A. Effect of the CLT

In [42] it was pointed out that for processes with independent increments, power law tails and finite variance the asymptotic convergence is obviously ruled by the CLT. We want here to show results showing the actual numerical behaviour of this convergence. Let us then consider a discrete process with independent increments x_i i.i.d. distributed according to a certain pdf $p(x_i)$ for all i such that

$$E[x_i] = 0, \;\; Var[x_i] = \sigma^2 \Delta t < \infty, \tag{17}$$

for some constant σ, where Δt is the time interval between two increments. Let us stress that we are not making any assumption on $p(x_i)$ which can be skewed, power law-tailed or both as long as the variance is finite. For example it could be the density of a shuffled empirical time-series. We now introduce the quantity

$$S_N = \sum_{i=1}^{N} x_i, \tag{18}$$

which is an the aggregated sum of N returns, thus

$$E[S_N] = 0, \;\; Var[S_N] = \sum_{i=1}^{N} Var[x_i] = \sigma^2 N \Delta t, \tag{19}$$

so the variance grows linearly with time as expected. We stress now that the quantity we use to measure the scaling of empirical time-series is exactly $E[|S_N|^q]$. In this case we are considering it for a shuffled/independent process.

The scaling properties of S_N are a straightforward consequence of the CLT. It can be shown (see A for an explicit computation) that

$$E[|S_\infty|^q] = \lim_{\substack{\Delta t \to 0 \\ N \to \infty \\ N\Delta t = \tau}} E[|S_N|^q] = \sigma^q \frac{2^{\frac{q}{2}}\Gamma(\frac{q+1}{2})}{\sqrt{\pi}} \tau^{\frac{q}{2}}. \tag{20}$$

Eq. 20 proves rigorously that any i.i.d. process with finite variance aggregates asymptotically into a unifractal process and in particular it scales as a BM (we underline that it holds also for shuffled empirical financial time-series). As a corollary, this also shows that empirical multifractality can arise only from a non trivial causal structure.

1. *First example: power law tails*

We apply here Eq. (20) to the case of tBM. For our purposes we chose the number of degrees of freedom (DoF) to be equal to $n = 3$ and, in order to remove as much noise as possible, we generated a time-series made of 10^7 steps. For a tBM Eq. (20) tells us everything about its asymptotic behaviour. In particular, with $n = 3$ and $q = 1$,

$$E[|S_\infty|] = \sqrt{\frac{6}{\pi}} \tau^{\frac{1}{2}}, \tag{21}$$

thus

$$\ln\left(E[|S_\infty|]\right) = \frac{1}{2}\ln(\tau) + \ln\left(\sqrt{\frac{6}{\pi}}\right). \tag{22}$$

In Fig. 1 we superpose the theoretical behaviour of Eq. (22) with the numerical one. As appears evident the linearity

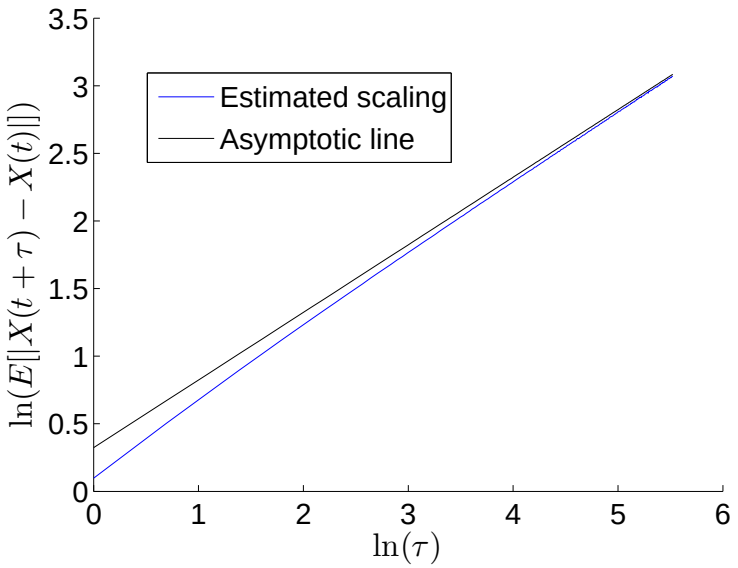

Figure 1: Blue solid line: numerical scaling of $E[|S_N|]$ for a tBM with $n = 3$ (cfr. Eq. (A3) with $q = 1$). Black solid line: theoretical expectation in the continuous limit.

is achieved only asymptotically (cfr. the effect of the productory in Eq. (A3)).

2. Second example: shuffled MRW

In this subsection we apply Eq. (20) in the case of shuffled MRW. We set the parameters to $\lambda = 0.3$, $L = 5000$ and $\sigma = 1$ (because of the shuffling the choice of the values of λ and L may be arbitrary while σ is simply a scale) and again we generated a time-series made of 10^7 steps to remove as much noise as possible. In Fig. 2 we superpose the theoretical behaviour of Eq. (20) with the numerical one for $q = 1$. As appears evident the linearity is achieved again

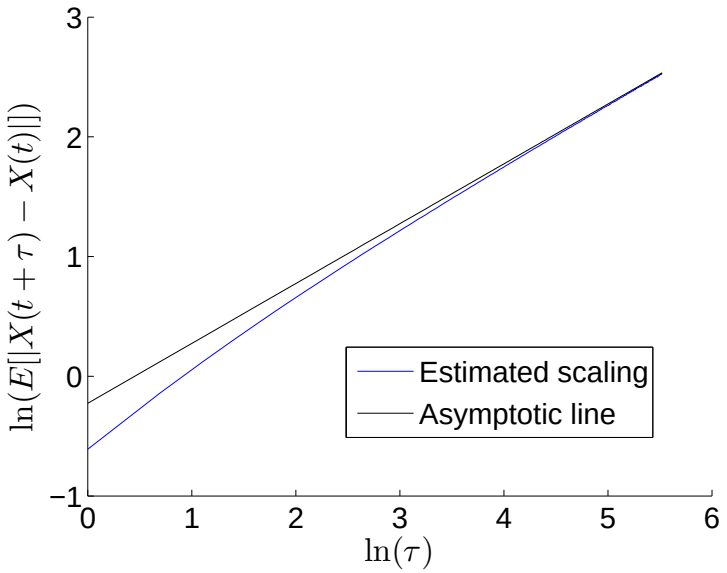

Figure 2: Blue solid line: numerical scaling of $E[|S_N|]$ for a shuffled MRW (cfr. Eq. (A3) with $q = 1$). Black solid line: theoretical expectation in the continuous limit.

only asymptotically (cfr. the effect of the productory in Eq. (A3)).

B. Effect of the autocorrelation

In [42] it is proven numerically that the autocorrelation is the true source of the empirical multifractality. In the same direction is the result of Subsec. IV A which proves that the shape of the distribution plays no role in the asymptotic scaling as long as the variance is finite. However for small aggregation horizons scaling measures are strongly biased also when the effect of the tails is removed (see [42]). These observations lead to the puzzling conclusion that the causal structure is, from the theoretical point of view, the source of the multifractal nature of a process, but, from a numerical point of view, also the source of a bias. In order to reconcile these results let us consider the case of the MRW. A first observations is that Eq. (16) holds in the continuous time limit whereas synthetic and real processes are inherently discrete in time. A second observation is that the innovations of the discretized version of the MRW, shown in Eq. (13), are conditionally Gaussian, whereas the distribution of the innovations in the continuous time limit has power law tails (cfr. [35]). It is worth noting that in this case continuous time limit means aggregating an infinite number of conditionally Gaussian variables with a certain memory structure given by Eq. (14). Thus, for the MRW, the mismatch arises because the discrete process in Eq. (13) is not a multifractal process described by the scaling exponents in Eq. (16), but its infinite aggregation limit (continuous time limit) is.
We propose that the same feature also holds for real financial processes, by arguing that the distribution of the returns at their smallest considered scale (for example tick-by-tick) is different from their distribution at large aggregations. For instance, one evident difference between returns taken on a tick-by-tick basis and, say, daily returns, is the role of the tick size ([63]). In the first case the returns have discrete values, while in the second case they can be safely modelled as continuous.
As a corollary of these observations, we observe that for the BM and the fBM the convergence issues are not present

because the distribution of the increments in the discrete version of the processes are Gaussian as the distribution of the increments in the continuous time limit *i.e.* they are described by a distribution stable under aggregation.

V. BUILDING A SCALING EXPONENTS PROXY

In this section we provide a procedure to estimate the scaling exponent of a given time-series. It is made up of two parts: the first consists in giving a reliable parameter free estimate of the set of scaling exponents taking into account the convergence issues discussed above, in the second, a fit of the measured scaling exponents is performed, allowing then to smooth them according to the theoretical prescriptions of the multifractal picture.

A. Taking into account the convergence issues

As shown in the previous section, the scaling properties of a time-series are completely uncovered only in the limit of infinite aggregation. In practical situations this condition is obviously unrealistic. In particular, for a process continuous in time, the condition of infinite aggregation of the increments is already satisfied at any finite aggregation horizon, while for a discrete time-series the infinite aggregation request translates into infinite aggregation horizon. It thus seems that the multifractal properties of a discrete time-series are theoretically uncovered only asymptotically. Let us consider then the logarithm of Eq. (4)

$$\ln\left(E[|X(t+\tau)-X(t)|^q]\right) = \zeta(q)\ln(\tau) + \ln\left(K(q)\right). \tag{23}$$

In [42] it was proven that the scaling measures are horizon dependent, in other words the results change with τ, reconciling with the theoretical expectations for large values of τ. It means in particular that the scaling is not exactly linear. In light of this we argue that for discrete processes the right hand side of Eq. (23) is an oblique asymptote. In other words, Eq. (23) holds exactly for every τ only for processes continuous in time, while for discrete ones a correction is needed due to the convergence issues. Let us define then $x = \ln(\tau)$ and $f(x) = \ln\left(E[|X(t+\tau)-X(t)|^q]\right)$ for a given value of q. Using these variables the usual fit performed in order to unveil the scaling structure of a time-series is

$$f(x) = mx + z \tag{24}$$

where then $m = \zeta(q)$ is the quantity we are interested in and z is the logarithm of the q-moment for $\tau = 1$. We propose now instead to take into account the convergence issues by generalizing Eq. (24) as

$$f(x) = g(x) + mx + z \tag{25}$$

where $g(x)$ is a correction function which we call filter function, which models the convergence toward the asymptotic behaviour. Coherently with the previous section, Eq. (25) has to satisfy the condition $g(x) \xrightarrow[x\to\infty]{} 0$. For real time-series, determining the actual shape of $g(x)$ is a hard task, however we developed a data driven method which allows to take into account the presence of $g(x)$ without computing it explicitly.

B. Taking advantage of the convergence issues

The first step is considering the integral of the signal. This implies that the scaling is now supposed to be given by the integral of Eq. (25), namely

$$F(x) = \int_0^x \left(g(x') + mx' + z\right) dx' = \int_0^x g(x')dx' + \frac{m}{2}x^2 + zx, \tag{26}$$

which is a parabola plus the integral of the filter function. Let us now assume that the filter function has a finite integral over the positive real axis[4], *i.e.*

$$\int_0^\infty g(x)dx = const, \tag{27}$$

[4] We recall that $g(x) \xrightarrow[x\to\infty]{} 0$ by definition, which is a necessary but not sufficient condition for the convergence of its integral.

which we will prove numerically in the next sections during applications. So it follows that

$$F(x) \xrightarrow[x\to\infty]{} \frac{m}{2}x^2 + zx + const. \tag{28}$$

We fit then the integrated empirical scaling with a parabolic shape, namely

$$p(x) = ax^2 + bx + c. \tag{29}$$

Theoretically it should be in perfect agreement with the empirical scaling in the interval[5] $[\tau^*, \infty)$ with $\tau^* \gg 1$. Varying then τ^* between 1 and ∞ we expect the term of degree zero in Eq. (29) *i.e.* $c(\tau^*)$, to reach asymptotically a plateau since it represents the area between the empirical scaling and the asymptotic linear scaling. Three scenarios are possible: if the empirical scaling tends to the asymptote from above, we expect $c(\tau^*)$ to be positive since the integral of the filter function is a positive number, if the empirical scaling tends to the asymptote from below, we expect $c(\tau^*)$ to be negative since the integral of the filter function is a negative number, if the empirical scaling oscillates around the asymptote before converging on it, we expect $c(\tau^*)$ to present maxima and minima.

C. Finding the maximum value of the aggregation

However due to the finiteness of empirical samples a maximum value of aggregation, τ_{max}, has to be found. Moreover, from a theoretical point of view the multifractal scaling holds only as long as the causal structure plays a role (cfr. [42]). In light of this we infer that a good proxy for the value of τ_{max} is the autocorrelation length. It is known (cfr. [58, 59]) that, given an iid discrete process of length T, say $|r_\tau(t)|^q$, its autocorrelation function behaves asymptotically as a normally distributed noise, $N(0, 1/T)$. In light of this, the most common choices for cutting its autocorrelation profile are:

1. the first lag when the autocorrelation function of $|r_\tau(t)|^q$ reaches the 99%th of the noise distribution,
2. the first lag when the autocorrelation function of $|r_\tau(t)|^q$ reaches the 95%th of the noise distribution,
3. the first lag when the autocorrelation function of $|r_\tau(t)|^q$ reaches the 50%th (zero level) of the noise distribution.

Since fixing one of these criteria would be arbitrary, for empirical data we apply all three prescriptions running our algorithm for all of them, deciding afterwards the best of the three using a criterion we discuss in a following subsection based on the root-mean-square error. We however report that in general, given a certain value of τ_{max}, it is always a good habit to check the empirical scaling in loglog scale and, if linearity does not hold, reduce τ_{max} accordingly.

D. Finding the minimum value of the aggregation

Let us now describe how the value of τ_{min} is fixed. Going back to the function $c(\tau^*)$, fixing a maximum value means that now finite size effects occur. In particular we found that when τ^* approaches τ_{max}, $c(\tau^*)$ starts to wildly oscillate because the number of points over which the fit is performed becomes too small. Thus we need to understand which value of $c(\tau^*)$ gives us a good approximation of its asymptotic behaviour, which in turn would give us information about τ_{min}. In principle we do not know if the empirical scaling will settle on its asymptote from above or below (maybe oscillating before), however we expect a good approximation of its asymptotic behaviour to be given either by one of its maxima, if it finally settles from above, or by one of its minima, if it finally settles from below. In order to make a statistically meaningful decision, we prescribe to take, among the set of all maxima and minima of $c(\tau^*)$, the one which attains the maximum value of the adjusted coefficient of determination [60]. We call the value of τ^* where this maximum/minimum occurs τ_{min}. In order to avoid the method to detect spurious maxima/minima) due to noise in the scaling we add the condition that the τ_{min} have to be such that $H(q) = 2a(\tau_{min})/q > 0.5$ to ensure the concavity of the function $\zeta(q)$. Once both the values of τ_{min} and τ_{max} are fixed, the best linear fit of the scaling of the considered moment can be performed in the range $[\tau_{min}, \tau_{max}]$, where the slope gives the value of scaling exponent itself.

[5] We recall that $x = \ln(\tau)$.

E. Fitting the scaling exponents

The procedure described up to now is completely parameter-free and allows to estimate single scaling exponents. In order to smooth the measured scaling exponents coherently with the multifractal picture requirement and to make a quantitative assessment about the overall shape of the empirical functions $\zeta(q)$, we decided to perform a polynomial robust fit, using the least absolute residuals method (see [61]), with q between -0.9 and 1 every 0.1 units, extending then the prescription given in [42]. In particular we used a second and a fourth degree polynomials[6]. Let us first consider the latter, namely

$$\zeta(q) = Dq^4 + Cq^3 + Bq^2 + Aq + const. \tag{30}$$

In its most general form Eq. (30) has 5 degrees of freedom, however, the function $\zeta(q)$ must satisfy few conditions, in particular

$$\begin{cases} \zeta(0) = 0 \\ \zeta(2) = 1 \\ \zeta''(q) < 0. \end{cases} \tag{31}$$

The first condition follows directly from the definition of the scaling exponents (see Subsec. II B), the second one, which implies $H(2) = 0.5$, follows from the absence of autocorrelation in the empirical financial returns (we give a simple proof of this in B), the third one follows from the concavity condition (cfr. Subsec. II B and references). Applying these conditions to Eq. (30), they become respectively (we report the explicit computation of the third condition in C)

$$\begin{cases} const = 0 \\ A = \dfrac{1}{2} - 8D - 4C - 2B \\ B = \dfrac{3C^2}{8D} \text{ with } D < 0, \end{cases} \tag{32}$$

so Eq. (30) can be rewritten as

$$\begin{cases} \zeta(q) = Dq^4 + Cq^3 + \dfrac{3C^2}{8D}q^2 + \left(\dfrac{1}{2} - 8D - 4C - \dfrac{3C^2}{4D}\right) q \\ D < 0, \end{cases} \tag{33}$$

which has only two degrees of freedom, *i.e.* C and D. As for the second degree polynomial fit, in its most general form it reads as

$$\zeta(q) = Bq^2 + Aq + const, \tag{34}$$

which then, enforcing conditions in Eq. (31), becomes

$$\begin{cases} \zeta(q) = Bq^2 + \left(\dfrac{1}{2} - 2B\right) q \\ B < 0, \end{cases} \tag{35}$$

having then only one degree of freedom. For each empirical time-series we chose between the two fits checking the maximum value of the adjusted coefficient of determination (see [60]). At this point we have then a shape for each of the three proposed autocorrelation lengths given in Subsec. V C. As a criterion to choose among them, we keep the fit which attains the least value of the root-mean-square error, in other words the one which leads to the least dispersion of the data around the fitted curve.

F. Summary of the method

1. Given one prescription for the autocorrelation length (see Subsec. V C), compute the value of τ_{max} for every measured q fixing then its value to be the maximum among them;

[6] The third degree is ruled out by the concavity requirement.

2. integrate the empirical scaling of the chosen qth absolute moments computed in $\tau \in [1, \tau_{max}]$;

3. for each moment fix the value of τ_{min} observing the behaviour of the term of degree zero of the parabolic fit (cfr. Eq. 29 and Subsec. V D);

4. infer the value of the scaling exponents via the best linear fit in the scaling regions $[\tau_{min}, \tau_{max}]$;

5. check that the filter function $g(x)$ converges to zero and that its integral converges to a constant;

6. perform a parabolic and a quartic fit, then decide the best among them checking the maximum adjusted coefficient of determination;

7. repeat steps from 1 to 6 for all three prescriptions for choosing τ_{max} (see Subse. V C) and select the one which gives the overall fit with the least root-mean-square error.

What it is left, is to prove that in the range $[\tau_{min}, \tau_{max}]$ chosen via this method, the filter function reaches a plateau, thus proving that its effect has been completely filtered out. This will be proved numerically in next sections. In particular we will show that this holds for the MRW, where the absolute moments scaling is computed for its increments (cfr. Eq. (13)), and afterwards for empirical data, where the absolute moments scaling is computed for the log-returns. We point out that for every τ we remove the mean from every return time-series since a non-zero mean would end up in the detection of spurious autocorrelations due also to possible non-stationarities. We report that this operation is justified by the financial assumption of zero returns on average.

VI. APPLICATION TO SYNTHETIC DATA: VALIDATION OF THE METHOD

In this section we show the application of the method on a MRW, which has known multifractal properties, proving the capability of our method to capture, for example, the expected values of $H(-0.5)$, $H(-0.3)$, $H(-0.1)$, $H(0.1)$, $H(0.5)$ and $H(1)$. As an example, in Fig. 3 are reported all the relevant steps of the application of the method for the computation of $H(1)$ to a MRW made of $N = 10^7$ steps, $\lambda = 0.3$, $L = 5000$ and $\sigma = 10^{-5}$. The length of the time-series was chosen to reduce as much as possible the noise, the value of λ to show clearly the convergence issues caused by the interplay between the power law tails and the volatility clustering while L and σ were chosen in order to be comparable with their value measured on empirical tick-by-tick financial data. In particular we report, from left to right from top to bottom, the integrated measured scaling (cfr. Eq. (26)), the whole shape of $c(\tau^*)$ and the maximum where the best parabolic fit is attained (cfr. Eqs. (28) and (29)), a zoom of the behaviour of $c(\tau^*)$ around the maximum where the best parabolic fit is attained (cfr. Eqs. (28) and (29)), the plain scaling with the asymptotic inferred scaling (cfr. Eqs. (23) and (25)), the filter function $g(x)$ and the integrated filter function (cfr. Eq. (27)). In order to choose the value of τ_{max} we fix it independently for each value of q using the cut of the autocorrelation at the 99% confidence level. As it appears evident from the figures, $c(\tau^*)$ reaches a first maximum and then starts to oscillate. The left bottom figures proves that the filter function converges to zero for high values of $x = \ln \tau$ while the right bottom one that its integral actually converges, thus filling the gaps left opened in the previous section at least for this particular process. The numerically computed scaling (blue solid line in the middle right figure) appears to settle on the asymptotic inferred scaling from above (dashed red line). In Fig. 4 we report instead the whole spectrum.

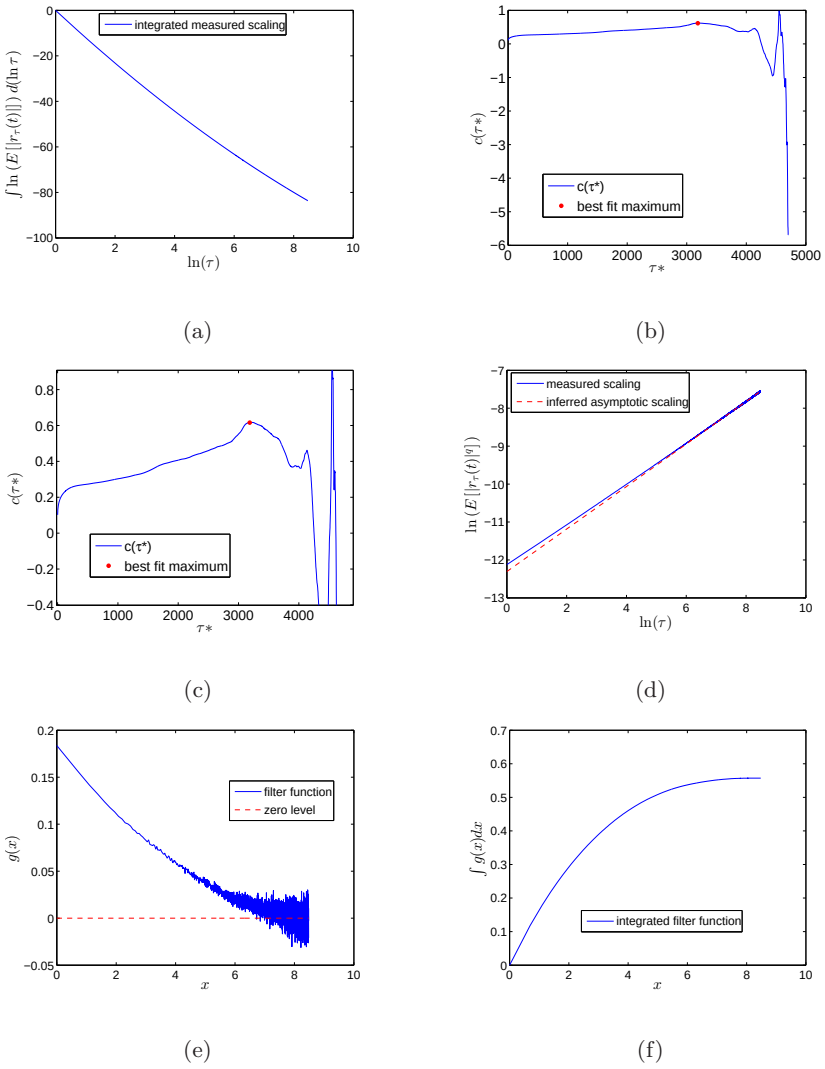

Figure 3: (a) integrated measured scaling (cfr. Eq. (26)). (b) in blue solid line $c(\tau^*)$ and the maximum where the best parabolic fit is attained marked with a red or shaded dot (cfr. Eqs. (28) and (29)). (c) zoom of the behaviour of $c(\tau^*)$ around the maximum where the best parabolic fit is attained (red or shaded dot) (cfr. Eqs. (28) and (29)). (d) plain scaling in blue solid line and the asymptotic inferred scaling in red dashed line (cfr. Eqs. (23) and (25)). (e) filter function $g(x)$ in blue solid line and the zero level in red dashed line. (f) integrated filter function (cfr. Eq. (27)).

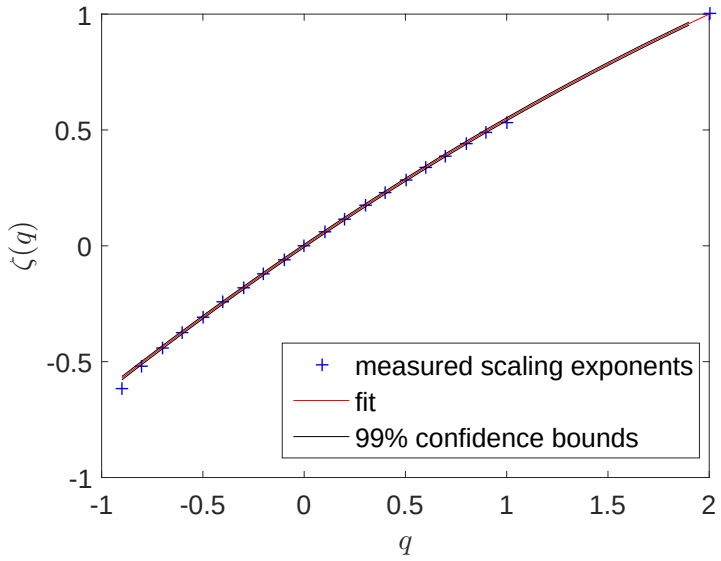

Figure 4: Fitted measured scaling exponents for a realization of a MRW. Blue crosses: measured scaling exponents. Red solid line: polynomial fit. Black solid lines: 99% confidence intervals of the values of the fitted curve.

In order to make a quantitative assessment we generated 10^4 MRWs made of 10^6 points and $\lambda = 0.3,\ 0.4, 0.5$, $L = 5000$, $\sigma = 10^{-5}$ as before. On each of them we applied our method in order to compute $H(-0.5)$, $H(-0.3)$, $H(-0.1)$, $H(0.1)$, $H(0.5)$, $H(1)$ and, since we found the estimators distributions are skewed, we report their median and median absolute deviation. We report the results in Tab. I along with the theoretical values between parenthesis in boldface under the measured values. The notation of the hat means the estimator of the quantity under it.

MRW	$\lambda = 0.3$	$\lambda = 0.4$	$\lambda = 0.5$
$\hat{H}(-0.5)$	0.612 ± 0.028 (**0.6125**)	0.696 ± 0.033 (**0.7**)	0.795 ± 0.042 (**0.8125**)
$\hat{H}(-0.3)$	0.607 ± 0.035 (**0.6035**)	0.680 ± 0.043 (**0.684**)	0.770 ± 0.047 (**0.7875**)
$\hat{H}(-0.1)$	0.597 ± 0.033 (**0.5945**)	0.665 ± 0.038 (**0.668**)	0.748 ± 0.042 (**0.7625**)
$\hat{H}(0.1)$	0.589 ± 0.031 (**0.5855**)	0.648 ± 0.033 (**0.652**)	0.725 ± 0.037 (**0.7375**)
$\hat{H}(0.5)$	0.569 ± 0.026 (**0.5675**)	0.617 ± 0.023 (**0.62**)	0.679 ± 0.029 (**0.6875**)
$\hat{H}(1)$	0.545 ± 0.023 (**0.545**)	0.577 ± 0.022 (**0.58**)	0.618 ± 0.024 (**0.625**)

Table I: Results of the application of the method in order to compute $H(-0.5)$, $H(-0.3)$, $H(-0.1)$, $H(0.1), H(0.5)$ and $H(1)$ of a MRW with parameters $\lambda = 0.3, 0.4, 0.5$ $L = 5000$, $\sigma = 10^{-5}$.

The measured values are in perfect agreement with the expected ones. In the next section we turn our attention to empirical data.

VII. APPLICATION TO REAL FINANCIAL DATA

In this section we discuss the application to real financial data. In particular we make few observations concerning the choice of the dataset, we illustrate the method step by step on a specific dataset while we show the final outcome

of its application to various other datasets.

A. The choice of the dataset

Nowadays trading takes place at high frequency speed which means that in a trading day may occur order of hundred thousands transactions. Moreover the number of transactions differs from day to day. As an example let us report the case of the trade log-price of the *American Express Company* (AXP), taken tick-by-tick from 12/10/2015 to 11/11/2015 traded on working days between 9:30 and 16:30 at the New York Stock Exchange (NYSE) made of 626710 points. The trading days in the given time-span are 23 and we can check for example how many trades occurred in the day with the minimum amount of trades and how many trades occurred in the day with the maximum amount of trades:

$$\begin{aligned} &\text{minimum } \# \text{ of trades} = 10110 \\ &\text{maximum } \# \text{ of trades} = 100133. \end{aligned} \tag{36}$$

In general we can say that, within a day, the secondly, minutely, hourly etc. returns are the result of the aggregation of the tick-by-tick returns (relative to the trading price). Thus if we consider the log price taken at a fixed time rate, say for example every second, it becomes a subordinated process which inherits the statistical properties of its subordinator (the trading time) (cfr. [62]), which we are in general not granted to be stationary. Moreover intraday data taken at a fixed time interval have strong seasonalities (cfr. [2]), which are instead almost absent in their tick-by-tick version. Seasonalities actually can also be avoided analysing daily data, however the subordination feature mentioned above still holds and also a long time span is required in order to proper measure the multifractal scaling (cfr. [42]). For example in order to obtain a time-series of roughly 25000 steps, around 100 years are needed, which heavily clashes with the assumption of stationarity. We add also that, according to our analyses, in order to reach a level of aggregation informative of the asymptotic behaviour, time-series made of at least 200000 steps are needed with an autocorrelation length of at least 1500 lags. Since these requirements are easily met by tick-by-tick data, we found quite a natural choice to limit our analysis to them. One last word has to be spent on the fact that in the tick-by-tick regime data are intrinsically discrete since in markets there is a lower bound to the fraction of the currency we trade with. We notice however that our analysis focuses on the high aggregation regime where the returns are supposed to take continuous values.

B. Numerical results: AXP

In this subsection we report the result of the application of our method for the computation of the scaling exponents of the AXP time-series, focusing in particular on $H(0.1)$ and $H(1)$ as an example. Given the prescription in Subsec. V C, the possible values of τ_{max} are

$$\begin{aligned} \tau_{max}^{99\%} &= 2798, \\ \tau_{max}^{95\%} &= 3507, \\ \tau_{max}^{50\%} &= 4201. \end{aligned} \tag{37}$$

According to the prescription of Subsec. V E the one which minimizes the dispersion of the data around the fitted curve is the first one, *i.e.* $\tau_{max} = 2798$. In Figs. 5 and 6 we report all the relevant steps for the computation of $H(0.1)$ and $H(1)$ as described in Sec. V B with the figures arranged as in Fig. 3. The empirical scaling appears to settle in both cases on the asymptotic straight line found by the algorithm (see Figs. 5 and 6) and the values of τ_{min} found are

$$\hat{\tau}_{min}^{H(0.1)} = 255, \;\; \hat{\tau}_{min}^{H(1)} = 815. \tag{38}$$

Again subfigures (e) and (f), in both cases, prove that, also for this empirical dataset, for high values of $x = \ln \tau$ the filter function $g(x)$ oscillates around zero and that its integral converges. We notice also that in Fig. 6 the choice of the local maximum may seem puzzling, since other apparently better candidates appear on its right. However we recall that the local maximum is chosen in order to achieve the best parabolic fit of the integrated scaling in the adjusted coefficient of determination sense. In order to complete our analysis of the scaling properties of the AXP time-series we report in Fig. 7 the fit of all the scaling exponents we measured. In this case we found a second degree

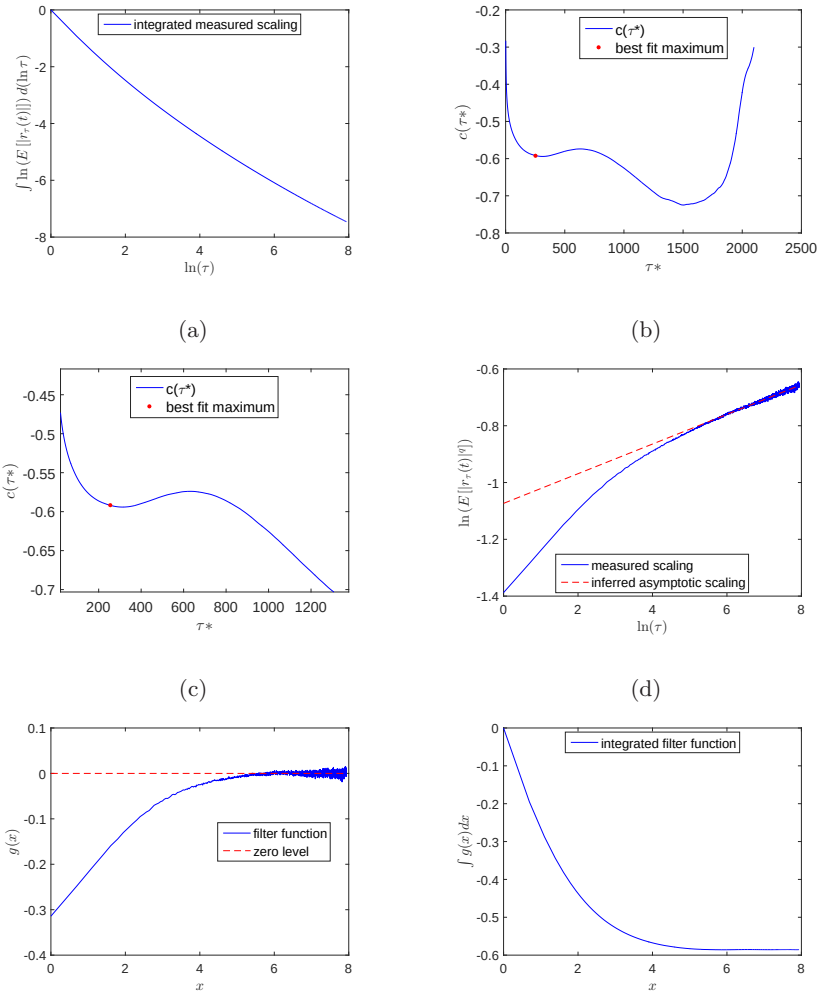

Figure 5: Step by step application of the method for the scaling of $H(0.1)$ for AXP. (a) integrated measured scaling (cfr. Eq. (26)). (b) in blue solid line $c(\tau^*)$ and the maximum where the best parabolic fit is attained marked with a red or shaded dot (cfr. Eqs. (28) and (29)). (c) zoom of the behaviour of $c(\tau^*)$ around the maximum where the best parabolic fit is attained (red or shaded dot) (cfr. Eqs. (28) and (29)). (d) plain scaling in blue solid line and the asymptotic inferred scaling in red dashed line (cfr. Eqs. (23) and (25)). (e) filter function $g(x)$ in blue solid line and the zero level in red dashed line. (f) integrated filter function (cfr. Eq. (27)).

polynomial fit to be appropriate with the coefficients equal to:

$$\hat{B} = -0.052 \quad (-0.058, -0.045), \tag{39}$$

where we reported in parenthesis the 95% confidence interval of the estimated coefficients.

C. Other data

In this section we report the application of the method to the following empirical time-series: Abbott Laboratories (ABT), AECOM (ACM), Adobe Systems (ADBE), American International Group (AIG), Advanced Micro Devices Inc. (AMD), Google (GOOGL), Honeywell International Inc. (HON), Marriott International (MAR), 3M Company (MMM), Procter & Gamble (PG). All time-series are taken between 12/10/2015 and 11/11/2015 on a tick-by-tick

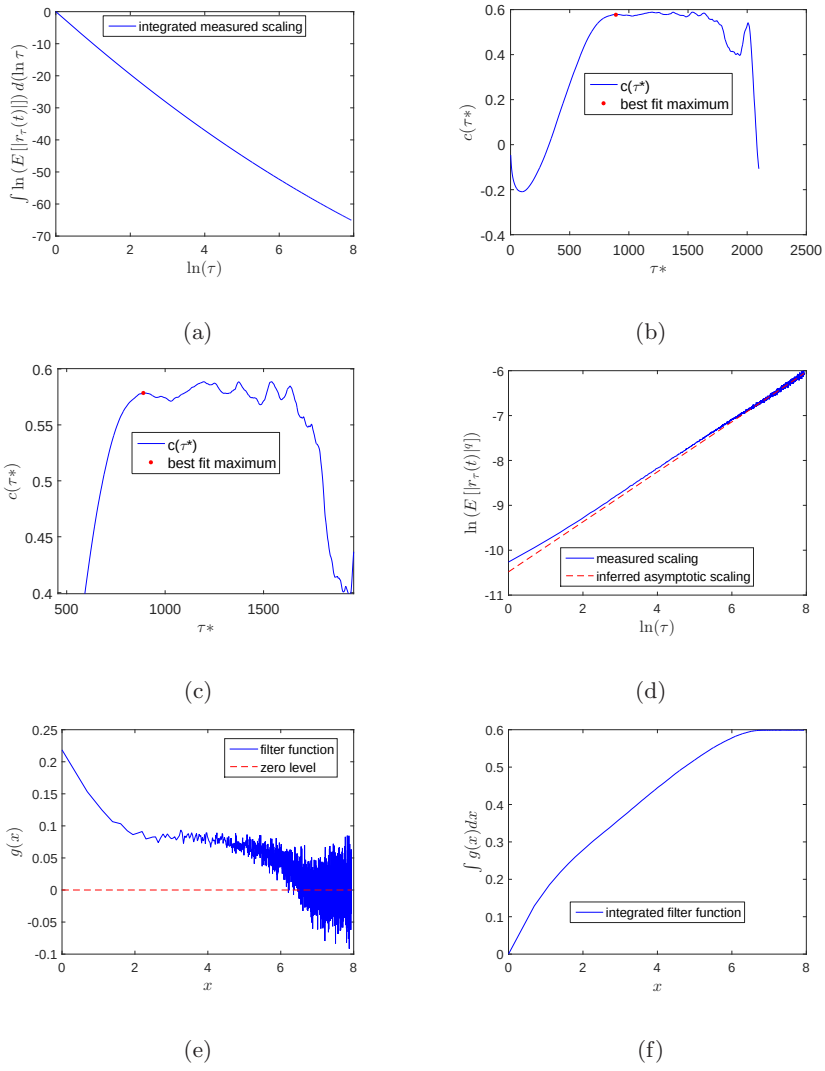

Figure 6: Step by step application of the method for the scaling of $H(1)$ for AXP. (a) integrated measured scaling (cfr. Eq. (26)). (b) in blue solid line $c(\tau^*)$ and the maximum where the best parabolic fit is attained marked with a red or shaded dot (cfr. Eqs. (28) and (29)). (c) zoom of the behaviour of $c(\tau^*)$ around the maximum where the best parabolic fit is attained (red or shaded dot) (cfr. Eqs. (28) and (29)). (d) plain scaling in blue solid line and the asymptotic inferred scaling in red dashed line (cfr. Eqs. (23) and (25)). (e) filter function $g(x)$ in blue solid line and the zero level in red dashed line. (f) integrated filter function (cfr. Eq. (27)).

basis and traded on the NYSE. Details concerning the length of each time-series, the values of τ_{max} and the application of the method are reported in Tab. II, along with the results of AXP discussed in the previous subsection. If we found a parabolic fit appropriate, the value of $\hat{B}$ is given, otherwise if we found a quartic fit appropriate, the values of $\hat{D}$ and $\hat{C}$ are given (see Subsec. V E) in both cases along with the 95% interval. In Figs. 8-17 we report instead for each empirical time-series the measured scaling exponents in blue crosses, the fitted polynomial in red solid line and the 99% confidence interval of the fitted functions in black solid lines. From Tab. II it appears that there is no clear preference for the parabolic or the quartic polynomial fit which is in turn linked to the complexity of the underlying generating process. For four time-series out of six for which the fourth degree polynomial is more suitable, we notice that the value of $\hat{C}$ can be assumed to be zero, which reflects in a symmetric Singularity Spectrum (cfr. Sec. II).

Ticker	$\hat{D}$	$\hat{C}$	$\hat{B}$	τ_{max}	# of points
ABT	/	/	$-0.0314(-0.0330, -0.0298)$	4761	733160
ACN	/	/	$-0.0185(-0.0198, -0.0173)$	2297	288564
ADBE	/	/	$-0.0125\ (-0.0157, -0.0092)$	3254	361922
AIG	$-0.0149(-0.0274, -0.0024)$	$0.0049(-0.02811, 0.038)$	/	8323	979380
AMD	$-0.0353(-0.0411, -0.0294)$	$0.1424(0.1325, 0.1523)$	/	1831	283456
AXP	/	/	$-0.0515(-0.0578, -0.0452)$	2798	626710
GOOGL	$-0.0524(-0.0535, -0.0512)$	$0.1404(0.1380, 0.1429)$	/	1904	237276
HON	/	/	$-0.0254(-0.0273, -0.0236)$	4692	444198
MAR	$-0.0055(-0.0077, -0.0032)$	$-0.0185(-0.0192, -0.0177)$	/	3504	317754
MMM	$-0.0091(-0.0121, -0.0061)$	$0.0065(-0.0028, 0.0158)$	/	2138	305018
PG	/	/	$-0.0622(-0.0642, -0.0601)$	4661	946435

Table II: Numerical results of the application of the method to empirical data. For each time-series is reported the ticker, the value of $\hat{D}$ and $\hat{C}$ or $\hat{B}$, whether we found more appropriate a second or a fourth degree polynomial fit, along with the 95% confidence interval, the value of τ_{max} and its length.

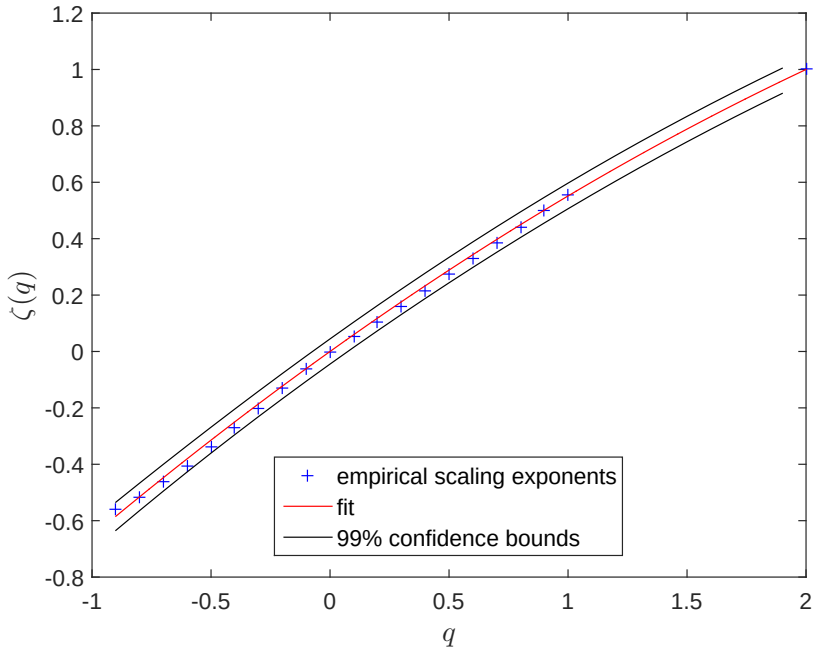

Figure 7: Blue crosses: empirical scaling exponents. Red solid line: polynomial fit. Black solid lines: 99% confidence intervals of the values of the fitted curve.

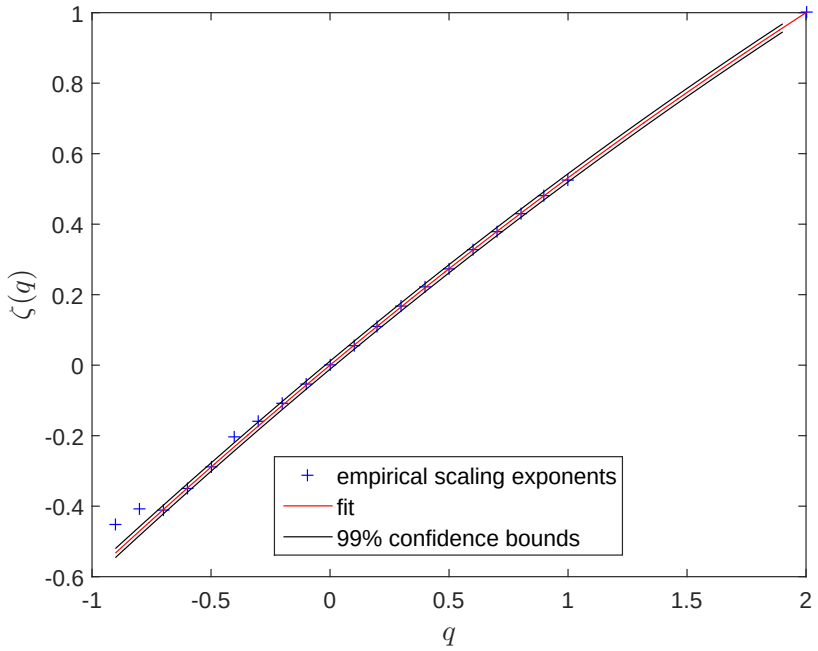

Figure 8: Fitted empirical scaling exponents for ABT time-series. Blue crosses: empirical scaling exponents. Red solid line: polynomial fit. Black solid lines: 99% confidence intervals of the values of the fitted curve.

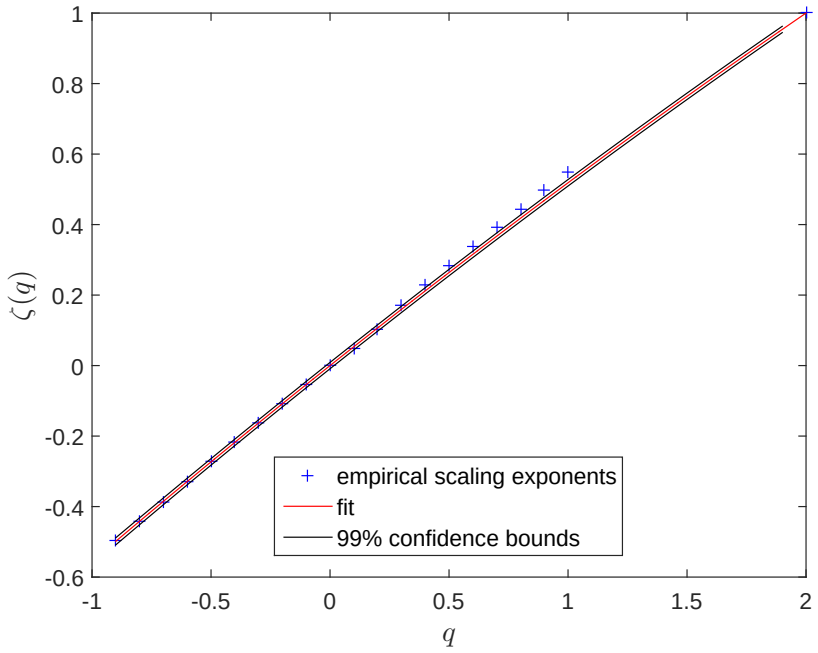

Figure 9: Fitted empirical scaling exponents for ACN time-series. Blue crosses: empirical scaling exponents. Red solid line: polynomial fit. Black solid lines: 99% confidence intervals of the values of the fitted curve.

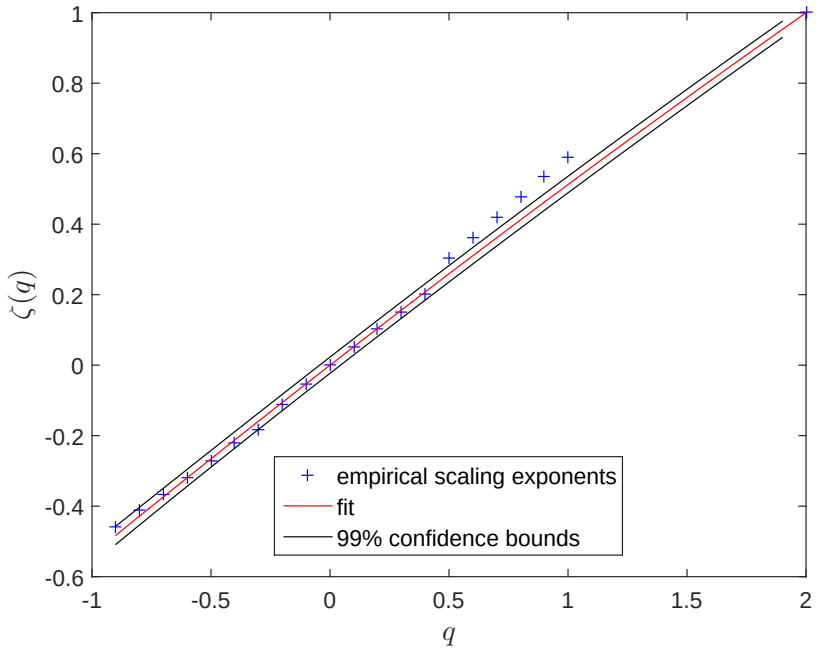

Figure 10: Fitted empirical scaling exponents for ADBE time-series. Blue crosses: empirical scaling exponents. Red solid line: polynomial fit. Black solid lines: 99% confidence intervals of the values of the fitted curve.

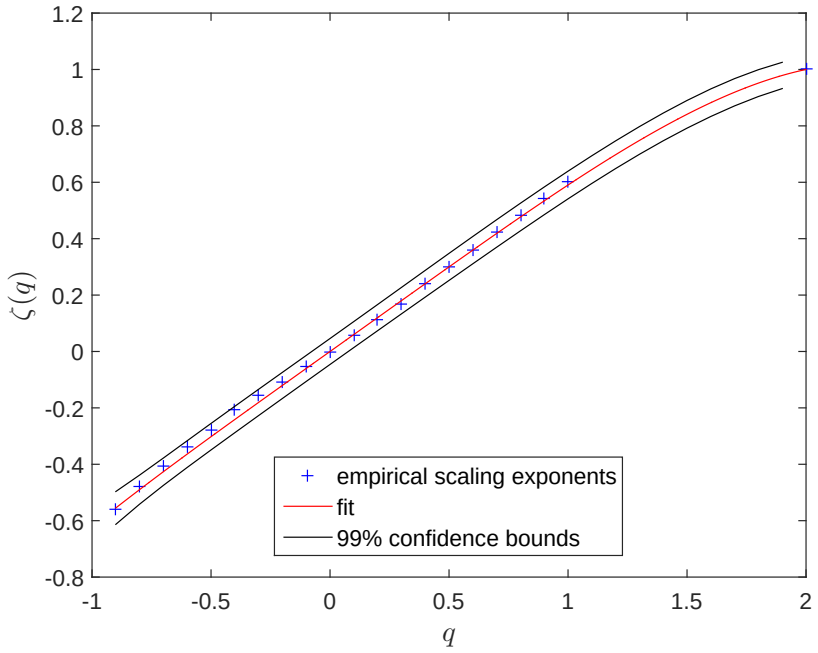

Figure 11: Fitted empirical scaling exponents for AIG time-series. Blue crosses: empirical scaling exponents. Red solid line: polynomial fit. Black solid lines: 99% confidence intervals of the values of the fitted curve.

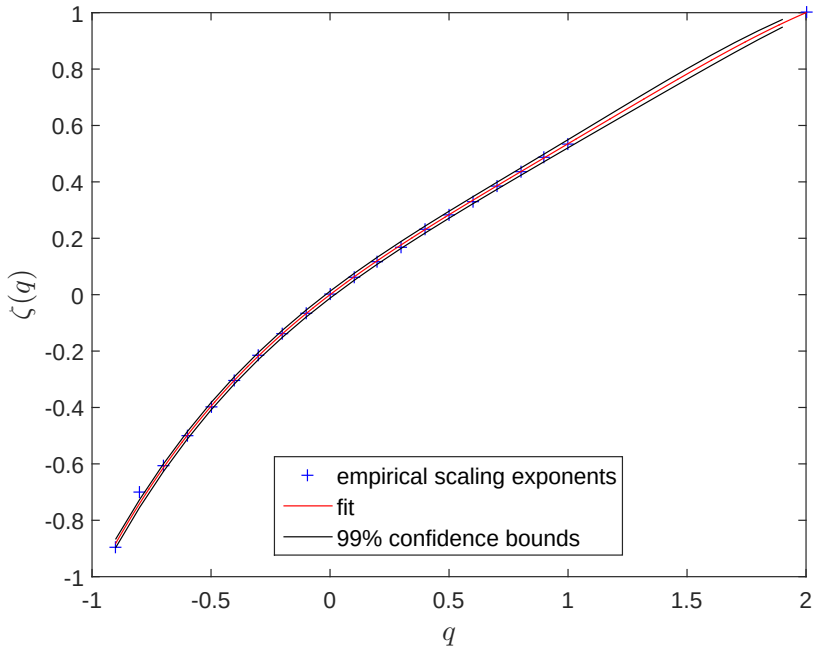

Figure 12: Fitted empirical scaling exponents for AMD time-series. Blue crosses: empirical scaling exponents. Red solid line: polynomial fit. Black solid lines: 99% confidence intervals of the values of the fitted curve.

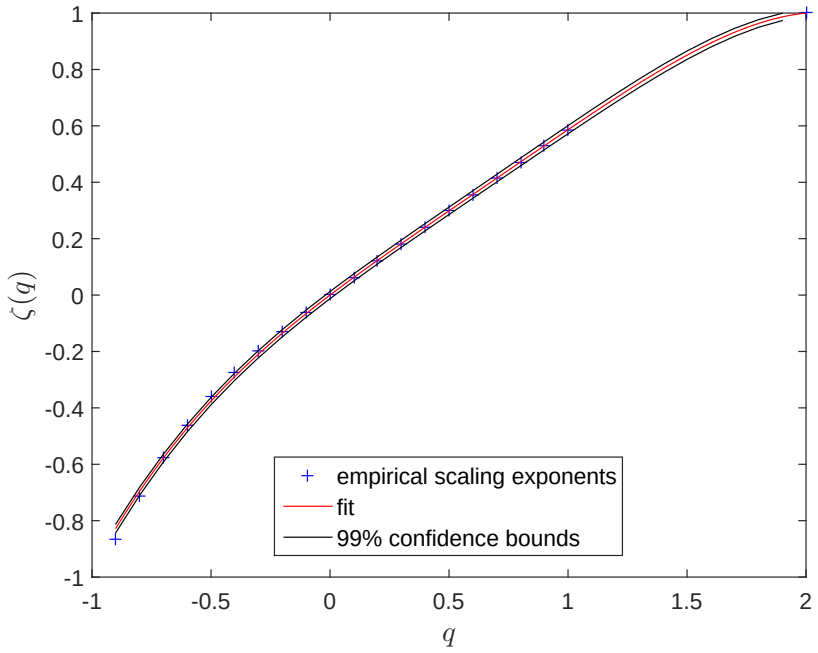

Figure 13: Fitted empirical scaling exponents for GOOGL time-series. Blue crosses: empirical scaling exponents. Red solid line: polynomial fit. Black solid lines: 99% confidence intervals of the values of the fitted curve.

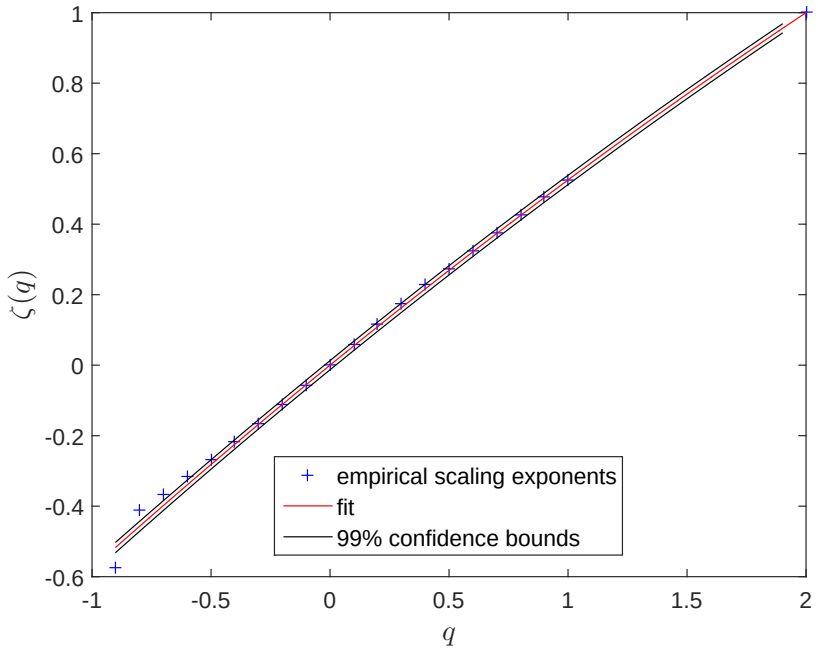

Figure 14: Fitted empirical scaling exponents for HON time-series. Blue crosses: empirical scaling exponents. Red solid line: polynomial fit. Black solid lines: 99% confidence intervals of the values of the fitted curve.

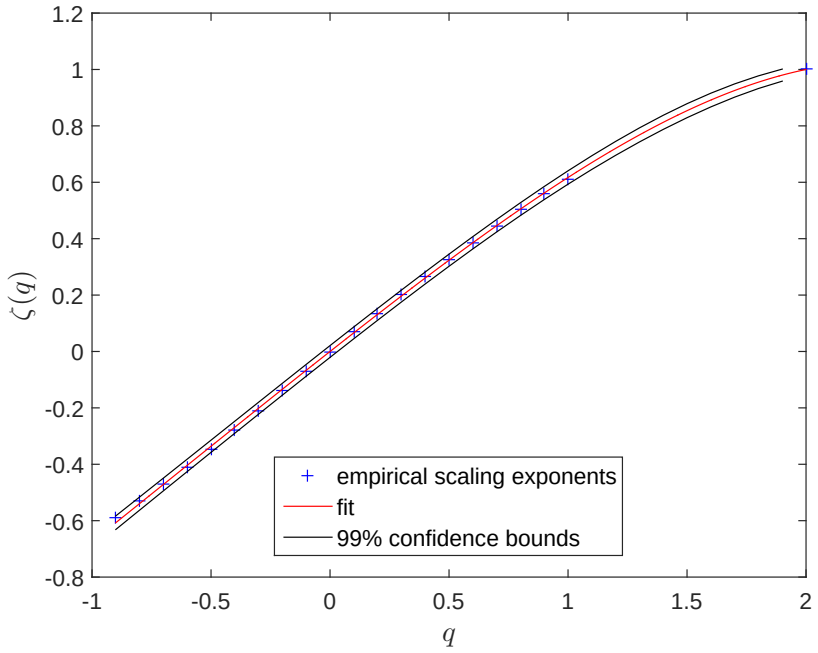

Figure 15: Fitted empirical scaling exponents for MAR time-series. Blue crosses: empirical scaling exponents. Red solid line: polynomial fit. Black solid lines: 99% confidence intervals of the values of the fitted curve.

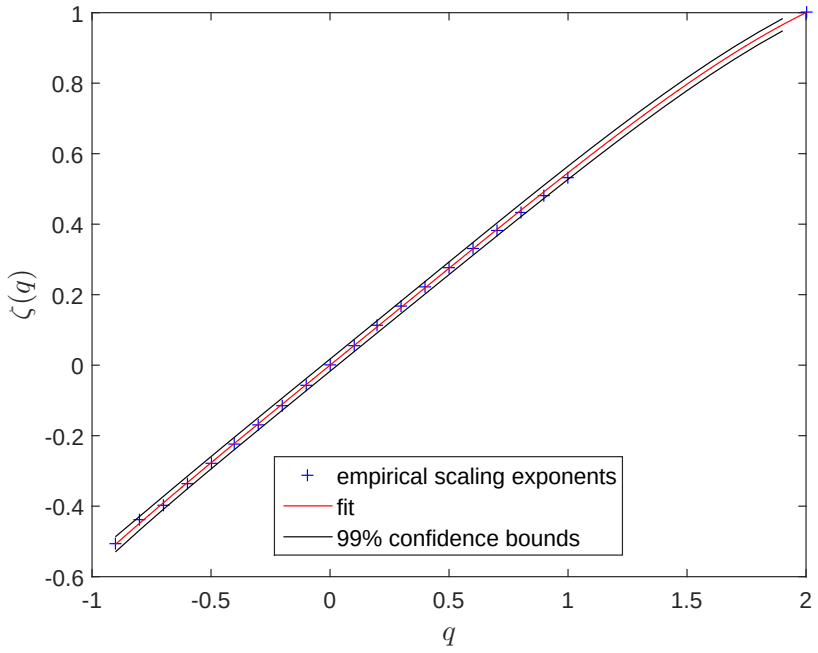

Figure 16: Fitted empirical scaling exponents for MMM time-series. Blue crosses: empirical scaling exponents. Red solid line: polynomial fit. Black solid lines: 99% confidence intervals of the values of the fitted curve.

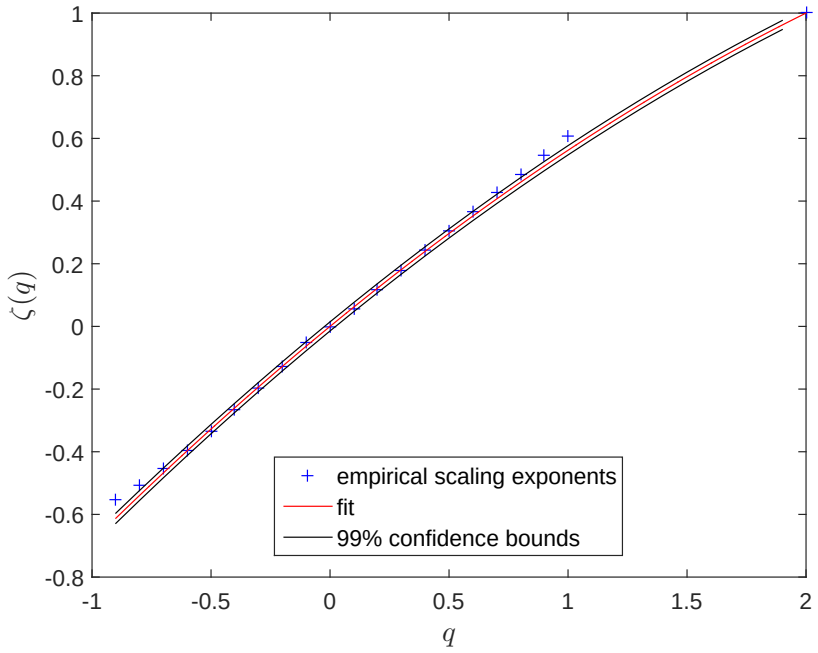

Figure 17: Fitted empirical scaling exponents for PG time-series. Blue crosses: empirical scaling exponents. Red solid line: polynomial fit. Black solid lines: 99% confidence intervals of the values of the fitted curve.

VIII. CONCLUSIONS

We proposed a new method to measure the scaling exponents of financial time-series, discussing how the discreteness of the available datasets, both for synthetic and real time-series, affects the scaling measures. In particular we showed that the exact power law scaling of the moments holds for multi/uni-scaling processes continuous in time, while it does not for their discrete counterparts and it appears to be recovered only in the high aggregation limit. We argued then that the scaling of discrete processes, which corresponds to a multi/uni-scaling process continuous in time, whether synthetic or real, should be corrected via a filter function. According to our interpretation of the results, the need of this filter function arises when a process is not stable under aggregation, which means that, for discrete processes, the distribution of the increments at the finest scale is different with respect to the one at gross scale *i.e.* in the continuous time limit. In order to circumvent this problem we devised a numerical method to subtract the filter function from the underlying linear scaling, without the need of knowing its exact functional form. Finally we smoothed the measured scaling exponents by fitting them with either a second or a fourth degree polynomial, which, taking into account the theoretical requirement of the multifractal picture, reduce to have respectively one and two degrees of freedom. In general terms, a higher degree corresponds to a higher degree of complexity of the underlying generating process.

We found that there are few qualitative features common to all stocks concerning the behaviour of the filter function. For positive moments, almost always the scaling clearly converges to the asymptotic behaviour found by our algorithm from above. However a different behaviour of the overall shape of the convergence is found for values of q near zero and values of q near one, with a transient between the two regimes. In particular for values of q near zero the empirical scaling crosses its asymptotic inferred behaviour from below finally settling on it from above, while, for all but one time-series (ABT), for q near one the empirical scaling stays always above the asymptotic one before settling on it again from above. From another perspective it means that positive absolute moments near to the first one tend to be always overestimated, whatever the aggregation, while small absolute moments tend to be underestimated for small aggregations while overestimated otherwise. As for the negative absolute moments the convergence pattern is stock-wise: in some cases the scaling lies always above the asymptotic scaling converging from above, in others it starts above, then it crosses the asymptotic scaling and finally converges from below. We report that this change of behaviour dependent on the order of the measured moment is absent for the MRW, where the convergence, for positive absolute moments, happens from above, while for negative ones it happens from below. We argue that this difference may arise from the fact that the innovations of a MRW, also at its finest scale, are (conditionally Gaussian) random variables continuous in value, whereas real financial tick-by-tick data are intrinsically discrete, due to the presence of

a minimum tick size (cfr. for example [63]). It is worth noting that this feature of tick-by-tick data does not affect the coherence of our work since the goal of our method is to measure the scaling behaviour in a high aggregation regime, where returns can be considered continuous in value. We stress that this convergence has been found in the so-called trading time, which is inhomogeneous. Different approaches has been developed to deal with time inhomogeneity of tick-by-tick data (see for example [2, 64, 65]), however we decided to avoid to introduce such techniques both because we performed a univariate analysis and because we preferred to avoid to introduce a source of arbitrariness coming from the choice of a specific procedure. Finally we report that as for the overall shape of the function $\zeta(q)$, we found that in our dataset there is no clear preference between the second or the fourth degree considered polynomials, despite in four cases out of six, where the fourth degree polynomial fit was found more suitable, the coefficient of the third degree term can be assumed to be zero within the error bounds.

For future developments we are planning to study the consequences of these considerations on the scaling in the physical time, which, making the time-series synchronous, would give us a natural setting in order to extend our approach to the study of the multivariate multifractality [66, 67].

ACKNOWLEDGEMENTS

The authors wish to thank Bloomberg for providing the data. T.D.M. wishes to thank the COST Action TD1210 for partially supporting this work. T.A. acknowledges support of the UK Economic and Social Research Council (ESRC) in funding the Systemic Risk Centre (ES/K002309/1).

Appendix A: Explicit computation of Eq. 20

In order to understand the scaling properties of the moments of S_N in the continuous time limit we need first to know its pdf S_N, namely $p_s(S_N)$. From the probability theory we know that this pdf is given by the convolution of the single pdfs. For example

$$\begin{aligned} p_s(S_2) = p(x_1) * p(x_2) = \int_{\mathbb{R}} dx_1 p(x_1) p(S_2 - x_1), \\ p_s(S_3) = p(x_1) * p(x_2) * p(x_3) = \int_{\mathbb{R}} dS_2 \int_{\mathbb{R}} dx_1 p(x_1) p(S_2 - x_1) p(S_3 - S_2). \end{aligned} \tag{A1}$$

In general, defining $S_0 = 0$,

$$p_s(S_N) = \prod_{i=1}^{N-1} \int_{\mathbb{R}} dS_i p(S_i - S_{i-1}) p(S_N - S_{N-1}). \tag{A2}$$

If we consider the discrete case what we usually compute after shuffling is

$$\begin{aligned} E[|S_N|^q] &= \int_{\mathbb{R}} dS_N |S_N|^q p_s(S_N) \\ &= \int_{\mathbb{R}} dS_N |S_N|^q \prod_{i=1}^{N-1} \int_{\mathbb{R}} dS_i p(S_i - S_{i-1}) p(S_N - S_{N-1}). \end{aligned} \tag{A3}$$

It is evident that the dependence of $E[|S_N|^q]$ from the time time-horizon $\tau = N\Delta t$ is certainly far from being a simple power law as requested by the multifractal picture (see Eq. (4)). Thus, this is why the numerical estimations are horizon-dependent. However analytically, in order to infer something about the multi/uni-scaling nature of the process x_i, we are interested in the continuous time limit of Eq. (A3), in line with the underling assumptions of multifractality. In particular we want to compute the simultaneous limits $\Delta t \to 0$, $N \to \infty$, but keeping the product $N\Delta t = \tau$ fixed, in order to have finite time horizons. In formulas we want to compute

$$\lim_{\substack{\Delta t \to 0 \\ N \to \infty \\ N\Delta t = \tau}} E[|S_N|^q] = E[|S_\infty|^q] = \lim_{\substack{\Delta t \to 0 \\ N \to \infty \\ N\Delta t = \tau}} \int_{\mathbb{R}} dS_N |S_N|^q p_s(S_N). \tag{A4}$$

Due to the CLT the following equality holds:

$$E[|S_\infty|^q] = \lim_{\substack{\Delta t\to 0\\ N\to\infty\\ N\Delta t=\tau}} \int_{\mathbb{R}} dS_N |S_N|^q \frac{e^{-\frac{S_N^2}{2\sigma^2 N\Delta t}}}{\sqrt{2\pi}\sigma\sqrt{N\Delta t}}. \tag{A5}$$

Using now the variable $z = \dfrac{S_N}{\sqrt{\sigma^2 N\Delta t}}$, Eq. (A5) becomes

$$E[|S_\infty|^q] = \lim_{\substack{\Delta t\to 0\\ N\to\infty\\ N\Delta t=\tau}} \int_{\mathbb{R}} dz \sigma^q (N\Delta t)^{\frac{q}{2}} |z|^q \frac{e^{-\frac{z^2}{2}}}{\sqrt{2\pi}}; \tag{A6}$$

Performing then the limit, taking out the constants and solving the integral (which is known), the solution is finally

$$E[|S_\infty|^q] = \sigma^q \frac{2^{\frac{q}{2}}\Gamma(\frac{q+1}{2})}{\sqrt{\pi}} \tau^{\frac{q}{2}}. \tag{A7}$$

Appendix B: Computation of the value of $H(2)$ of real financial processes

In this appendix we show that for empirical financial time-series $H(2) = 0.5$. As noted in [42], on empirical financial datasets the estimator of $H(2)$ cannot be reliably measured because the second moment of the empirical distributions is finite, but the fourth momentum is often infinite (cfr. [5, 46]).Using empirical evidence is however possible to infer its value in the limit of infinite aggregation. This simple result follows from the following properties of financial time-series, calling $r_\tau(t)$ the log-returns:

$$\begin{cases} E[r_\tau(t)] = 0 \\ Var[r_\tau(t)] < \infty \\ Corr[r_\tau(t_1), r_\tau(t_2)] = 0 \qquad t_1 \neq t_2. \end{cases} \tag{B1}$$

where by $Corr$ we mean the correlation function. We notice that in the high frequency domain the third property is true after few lags ([2, 5]) thus it does not affect the asymptotic properties of the scaling. Let us call then $\varepsilon_{\Delta t}(k)$ the elementary increments of a process satisfying the properties listed in Eq. (B1) with variance $Var[\varepsilon_{\Delta t}(k)] = \sigma^2\Delta t$, where σ is a fixed scalar and Δt the discretization step. The returns of this process under aggregation can be written on scale τ as

$$r_\tau(t) = \sum_{k=\frac{t}{\Delta t}+1}^{\frac{t+\tau}{\Delta t}} \varepsilon_{\Delta t}(k). \tag{B2}$$

The following chain of equalities hold

$$\begin{aligned} E[|r_\tau(t)|^2] &= Var[r_\tau(t)] = Var[\textstyle\sum_{k=\frac{t}{\Delta t}+1}^{\frac{t+\tau}{\Delta t}} \varepsilon_{\Delta t}(k)] \\ &= \sum_{k=\frac{t}{\Delta t}+1}^{\frac{t+\tau}{\Delta t}} Var[\varepsilon_{\Delta t}(k)]] + \sum_{k_1<k_2=\frac{t}{\Delta t}+1}^{\frac{t+\tau}{\Delta t}} 2Cov[\varepsilon_{\Delta t}(k_1), \varepsilon_{\Delta t}(k_2)] \\ &= \sigma^2\tau, \end{aligned} \tag{B3}$$

where the first and fourth equality follow from Eq. (B1). Thus, with the notation of Eq. (4), it can be written that

$$E[|r_\tau(t)|^2] = K(2)\tau^{2H(2)} = \sigma^2\tau; \tag{B4}$$

which in turn implies that $H(2) = 0.5$.

Appendix C: Effect of the concavity on the scaling exponents fitting function

In this appendix we derive the third condition in Eq. (32). The second derivative of Eq. (30) reads as

$$\zeta''(q) = 12Dq^2 + 6Cq + 2B. \tag{C1}$$

To ensure that the condition $\zeta''(q) < 0$ holds for every q the roots of (C1) must coincide and $D < 0$. In particular the roots of (C1) are

$$q_{\pm} = \frac{-3C \pm \sqrt{9C^2 - 24BD}}{12D}, \tag{C2}$$

which, in order to coincide, must satisfy

$$B = \frac{3C^2}{8D}. \tag{C3}$$

[1] R.N. Mantegna and H.E. Stanley. Introduction to Econophysics: Correlations and Complexity in Finance. Cambridge University Press, 1999.

[2] Michel M. Dacorogna, Ramazan Gençay, Ulrich A. Müller, Richard B. Olsen, and Olivier V. Pictet. An Introduction to High-Frequency Finance. Academic Press, San Diego, 2001.

[3] Rosario N Mantegna and H Eugene Stanley. Scaling behaviour in the dynamics of an economic index. Nature, 376(6535):46–49, 1995.

[4] Tiziana Di Matteo. Multi-scaling in finance. Quantitative finance, 7(1):21–36, 2007.

[5] Rama Cont. Empirical properties of asset returns: stylized facts and statistical issues. Quantitative Finance, 1(2):223–236, 2001.

[6] Shoaleh Ghashghaie, Wolfgang Breymann, Joachim Peinke, Peter Talkner, and Yadollah Dodge. Turbulent cascades in foreign exchange markets. Nature, 381(6585):767–770, 1996.

[7] Laurent E. Calvet and Adlai Fisher. Multifractality in asset returns: Theory and evidence. Review of Economics and Statistics, 84(3):381–406, 2002.

[8] Ruipeng Liu, Tiziana Di Matteo, and Thomas Lux. Multifractality and long-range dependence of asset returns: The scaling behaviour of the markov-switching multifractal model with lognormal volatility components. Kiel Working Papers, (1427), 2008.

[9] Marco Bartolozzi, Christopher Mellen, Tiziana Di Matteo, and Tomaso Aste. Multi-scale correlations in different futures markets. The European Physical Journal B-Condensed Matter and Complex Systems, 58(2):207–220, 2007.

[10] M. Bartolozzi, C. Mellen, F. Chan, D. Oliver, T. Di Matteo, and T. Aste. Applications of physical methods in high-frequency futures markets. Proc. SPIE, 6802:680203–680203–14, 2007.

[11] Ladislav Kristoukek. Fractal markets hypothesis and the global financial crisis: scaling, investment horizons and liquidity. Advances in Complex Systems, 15(06):1250065, 2012.

[12] Zhi-Qiang Jiang and Wei-Xing Zhou. Multifractality in stock indexes: Fact or fiction? Physica A: Statistical Mechanics and its Applications, 387(14):3605–3614, 2008.

[13] Thomas Lux. Detecting multi-fractal properties in asset returns: The failure of the scaling estimator. International Journal of Modern Physics C, 15(04):481–491, 2004.

[14] Dariusz Grech and Zygmunt Mazur. On the scaling ranges of detrended fluctuation analysis for long-term memory correlated short series of data. Physica A: Statistical Mechanics and its Applications, 392(10):2384–2397, 2013.

[15] Dariusz Grech and Zygmunt Mazur. Scaling range of power laws that originate from fluctuation analysis. Physical Review E, 87(5):052809, 2013.

[16] LG Moyano, J De Souza, and SM Duarte Queirós. Multi-fractal structure of traded volume in financial markets. Physica A: Statistical Mechanics and its Applications, 371(1):118–121, 2006.

[17] Jeferson de Souza and Sílvio M. Duarte Queirós. Effective multifractal features of high-frequency price fluctuations time series and ℓ-variability diagrams. Chaos, Solitons & Fractals, 42(4):2512 – 2521, 2009.

[18] Raffaello Morales, T Di Matteo, Ruggero Gramatica, and Tomaso Aste. Dynamical generalized hurst exponent as a tool to monitor unstable periods in financial time series. Physica A: Statistical Mechanics and its Applications, 2012.

[19] Wei-Xing Zhou. Multifractal detrended cross-correlation analysis for two nonstationary signals. Physical Review E, 77(6):066211, 2008.

[20] Gao-Feng Gu and Wei-Xing Zhou. Detrending moving average algorithm for multifractals. Physical Review E, 82(1):011136, 2010.

[21] Wei-Xing Zhou. Finite-size effect and the components of multifractality in financial volatility. Chaos, Solitons & Fractals, 45(2):147–155, 2012.

[22] Noemi Nava, T. Di Matteo, and Tomaso Aste. Time-dependent scaling patters in high frequency financial data. The Eurpean Physical Journal Special Topics, 2016 (in press).
[23] Noemi Nava, T. Di Matteo, and Tomaso Aste. Anomalous volatility scaling in high frequency financial data. Physica A: Statistical Mechanics and its Applications, 447:434 – 445, 2016.
[24] Laurent E Calvet, Adlai J Fisher, and Benoit B Mandelbrot. A multifractal model of asset returns. Cowles Foundation Discussion Paper No. 1164, (1164), 1997.
[25] Laurent E. Calvet and Adlai Fisher. Forecasting multifractal volatility. Journal of Econometrics, 105(1):27–58, 2001.
[26] Thomas Lux. The markov-switching multifractal model of asset returns: Gmm estimation and linear forecasting of volatility. Journal of Business & Economic Statistics, 26(2):194–210, 2008.
[27] Thomas Lux and Leonardo Morales-Arias. Forecasting volatility under fractality, regime-switching, long memory and student- innovations. Computational Statistics & Data Analysis, 54(11):2676 – 2692, 2010. The Fifth Special Issue on Computational Econometrics.
[28] M. Segnon and T. Lux. Multifractal Models in Finance: Their Origin, Properties, and Applications. Kiel working paper. 2013.
[29] Ruipeng Liu, Tiziana Di Matteo, and Thomas Lux. True and apparent scaling: The proximity of the markov-switching multifractal model to long-range dependence. Physica A: Statistical Mechanics and its Applications, 383(1):35–42, 2007.
[30] Emmanuel Bacry, J Delour, and Jean-François Muzy. Multifractal random walk. Physical Review E, 64(2):026103, 2001.
[31] Jean-François Muzy and Emmanuel Bacry. Multifractal stationary random measures and multifractal random walks with log infinitely divisible scaling laws. Physical Review E, 66(5):056121, 2002.
[32] Emmanuel Bacry and Jean François Muzy. Log-infinitely divisible multifractal processes. Communications in Mathematical Physics, 236(3):449–475, 2003.
[33] Emmanuel Bacry, Laurent Duvernet, and Jean-François Muzy. Continuous-time skewed multifractal processes as a model for financial returns. Journal of Applied Probability, 49(2):482–502, 2012.
[34] Laurent E Calvet and Adlai J Fisher. How to forecast long-run volatility: Regime switching and the estimation of multifractal processes. Journal of Financial Econometrics, 2(1):49–83, 2004.
[35] Emmanuel Bacry, Alexey Kozhemyak, and Jean-François Muzy. Continuous cascade models for asset returns. Journal of Economic Dynamics and Control, 32(1):156–199, 2008.
[36] E. Bacry, A. Kozhemyak, and J. F. Muzy. Log-normal continuous cascade model of asset returns: aggregation properties and estimation. Quantitative Finance, 13(5):795–818, 2013.
[37] Jan W Kantelhardt, Stephan A Zschiegner, Eva Koscielny-Bunde, Shlomo Havlin, Armin Bunde, and H Eugene Stanley. Multifractal detrended fluctuation analysis of nonstationary time series. Physica A: Statistical Mechanics and its Applications, 316(1):87–114, 2002.
[38] Tiziana Di Matteo, Tomaso Aste, and MM Dacorogna. Scaling behaviors in differently developed markets. Physica A: Statistical Mechanics and its Applications, 324(1):183–188, 2003.
[39] T Di Matteo, T Aste, and Michel M Dacorogna. Long-term memories of developed and emerging markets: Using the scaling analysis to characterize their stage of development. Journal of Banking & Finance, 29(4):827–851, 2005.
[40] Jozef Barunik and Ladislav Kristoufek. On hurst exponent estimation under heavy-tailed distributions. Physica A: Statistical Mechanics and its Applications, 389(18):3844–3855, 2010.
[41] Alain Arneodo, E Bacry, and JF Muzy. The thermodynamics of fractals revisited with wavelets. Physica A: Statistical Mechanics and its Applications, 213(1):232–275, 1995.
[42] Riccardo Junior Buonocore, Tomaso Aste, and Tiziana Di Matteo. Measuring multiscaling in financial time-series. Chaos, Solitons & Fractals, 2015.
[43] Wei-Xing Zhou. The components of empirical multifractality in financial returns. EPL (Europhysics Letters), 88(2):28004, 2009.
[44] Jozef Barunik, T Aste, T Di Matteo, and Ruipeng Liu. Understanding the source of multifractality in financial markets. Physica A, 391:4234, 2012.
[45] Elena Green, William Hanan, and Daniel Heffernan. The origins of multifractality in financial time series and the effect of extreme events. The European Physical Journal B, 87(6):1–9, 2014.
[46] Anirban Chakraborti, Ioane Muni Toke, Marco Patriarca, and Frédéric Abergel. Econophysics review: I. empirical facts. Quantitative Finance, 11(7):991–1012, 2011.
[47] Laurent E. Calvet, Adlai Fisher, and Benoit Mandelbrot. Large deviations and the distribution of price changes. Cowles Foundation Discussion Paper No. 1165, 1997.
[48] Thomas C. Halsey, Mogens H. Jensen, Leo P. Kadanoff, Itamar Procaccia, and Boris I. Shraiman. Fractal measures and their singularities: The characterization of strange sets. Phys. Rev. A, 33:1141–1151, Feb 1986.
[49] R Benzi, G Paladin, G Parisi, and A Vulpiani. On the multifractal nature of fully developed turbulence and chaotic systems. Journal of Physics A: Mathematical and General, 17(18):3521, 1984.
[50] R. Benzi, G. Parisi, and Società italiana di fisica. Turbulence and Predictability in Geophysical Fluid Dynamics and Climate Dynamics: Proceedings of the International School of Physics "Enrico Fermi," Course LXXXVIII, Varenna on Lake Como, Villa Monastero, 14-24 June 1983. North-Holland, 1985.
[51] Laurent E Calvet, Adlai J Fisher, and Benoit B Mandelbrot. Multifractality of deutschemark/us dollar exchange rates. Cowles Foundation Discussion Paper No. 1166, (1166), 1997.
[52] Albert-László Barabási and Tamás Vicsek. Multifractality of self-affine fractals. Physical Review A, 44(4):2730, 1991.
[53] N.L. Johnson, S. Kotz, and N. Balakrishnan. Continuous univariate distributions. Number v. 2 in Wiley series in probability and mathematical statistics: Applied probability and statistics. Wiley & Sons, 1995.

[54] Hiroya Nakao. Multi-scaling properties of truncated lévy flights. Physics Letters A, 266(4):282–289, 2000.
[55] A.V Chechkin and V.Yu Gonchar. Self and spurious multi-affinity of ordinary levy motion, and pseudo-gaussian relations. Chaos, Solitons & Fractals, 11(14):2379 – 2390, 2000.
[56] Karim Abadir and Jan Magnus. The central limit theorem for student's distribution—solution. Econometric Theory, 20(06):1261–1263, 2004.
[57] E Bacry, J Delour, and JF Muzy. Modelling financial time series using multifractal random walks. Physica A: Statistical Mechanics and its Applications, 299(1):84–92, 2001.
[58] M. S. Bartlett. On the theoretical specification and sampling properties of autocorrelated time-series. Supplement to the Journal of the Royal Statistical Society, 8(1):27–41, 1946.
[59] Zhuanxin Ding, Clive W.J. Granger, and Robert F. Engle. A long memory property of stock market returns and a new model. Journal of Empirical Finance, 1(1):83 – 106, 1993.
[60] Henri Theil. Economic forecasts and policy. Amsterdam : North-Holland Pub. Co, 2nd rev. ed edition, 1961. Includes bibliographical references.
[61] Peter Bloomfield and William Steiger. Least absolute deviations curve-fitting. SIAM Journal on Scientific and Statistical Computing, 1(2):290–301, 1980.
[62] B.B. Mandelbrot, P.H. Cootner, R.E. Gomory, E.F. Fama, W.S. Morris, and H.M. Taylor. Fractals and Scaling in Finance: Discontinuity, Concentration, Risk. Selecta Volume E. SpringerLink : Bücher. Springer New York, 2013.
[63] Jean-Philippe Bouchaud, Marc Mézard, Marc Potters, et al. Statistical properties of stock order books: empirical results and models. Quantitative finance, 2(4):251–256, 2002.
[64] Jeffrey R. Russel and Robert F. Engle. Analysis of high frequency financial data, chapter 7, pages 383–426. Handbooks in Finance. Elsevier Science, 2009.
[65] Alexandre Dupuis and Richard B. Olsen. High Frequency Finance: Using Scaling Laws to Build Trading Models, pages 563–584. John Wiley & Sons, Inc., 2012.
[66] Charles Meneveau, KR Sreenivasan, P Kailasnath, and MS Fan. Joint multifractal measures: Theory and applications to turbulence. Physical Review A, 41(2):894, 1990.
[67] Wen-Jie Xie, Zhi-Qiang Jiang, Gao-Feng Gu, Xiong Xiong, and Wei-Xing Zhou. Joint multifractal analysis based on the partition function approach: analytical analysis, numerical simulation and empirical application. New Journal of Physics, 17(10):103020, 2015.